

Intramolecular changes during polymorphic transformations of amylose

A. D. French and V. G. Murphy†

Southern Regional Research Center‡, New Orleans, Louisiana, USA

(Received 29 November 1976; revised 5 January 1977)

A survey of small saccharide crystal structures indicates that there is substantial variability in the shape of the α -D-glucose residue and in the conformation angles at the glycosidic linkage. Both factors appear to be altered primarily by hydrogen bonding and crystal packing forces. For the purposes of building computer models of cyclodextrins and amyloses, the residues from different crystals may be characterized in terms of the virtual angles, O(1)–C(1)–C(4) and C(1)–C(4)–O(4). Computer models of six-, seven-, and eight-residue cyclodextrins require residues having different such angular values because of the role played by the parameter n (number of residues per cycle). In computer models of amyloses, a similar role is also played by the helical parameter h (rise per residue). It is therefore concluded that polymorphic transformations often involve alterations in monomeric geometry as well as rotations about valence bonds to the linkage oxygen atoms. Finally, it is proposed that the entire space of accessible conformations be represented on a grid of h vs. n with consideration given to the full range of residue geometries at each grid point.

INTRODUCTION

The starch fraction, amylose, is of interest because, in addition to its commercial importance, it is known to crystallize in a wide variety of molecular conformations. Amylose is also important to those who study polysaccharides because of the wealth of relevant information available. For example, single crystal diffraction studies have yielded more than 100 determinations of the monomeric geometry, and many of these studies have been on molecules that possess the amylosic (1 α ,4 e) glycosidic linkage. Conclusions from this mass of crystallographic information are that the glucose ring is flexible within the constraints of the 4C_1 conformation and that there is substantial variability in the bond and torsion angles at the glycosidic linkage.

We previously showed that it is necessary to draw upon different glucose geometries in order to construct satisfactory computer models of various known polymorphs of amylose¹. A corollary to that idea is now proposed, viz. that a change in residue geometry is often one of the characteristics of a polymorphic transformation. A theory of helical constraints is derived and tested with single crystal data from cycloamyloses, which have 'helical' constraints, and maltoses, which do not. Then, taking note of the systematic nature of the required changes in residue geometry imposed by helical constraints, models for all the known polymorphs of amylose are presented. These models have differences in both the residue geometry and the linkage conformation angles; consequently, a new representation of accessible conformation space seems required and is proposed herein.

* Presented at the First Cleveland Symposium on Macromolecules, Structure and Properties of Biopolymers, Case Western Reserve University, Cleveland, Ohio, USA, October 1976.

† Present address: Department of Chemical Engineering, Iowa State University, Ames, Iowa, USA.

‡ One of the facilities of the Southern Region, Agricultural Research Service, United States Department of Agriculture.

STEREOCHEMICAL SURVEY

The range of residue geometry available at the time of our previous study¹ has been expanded. The individual conformation angles of the glucose rings are now observed to vary as much as 20°, and the O(4)–O(1) distance ranges down to 4.05 Å. The latter value is for the non-reducing residue from α -maltose monohydrate² and may be contrasted with 4.57 Å for the 'non-reducing' residue from methyl β -maltoside monohydrate³, which is at the upper end of the range. Despite the 0.52 Å variability in O(4)–O(1) distance, the distance between C(1) and C(4) is 2.88 Å \pm 0.03 Å in many accurately determined structures. This constancy, coupled with the variability in O(4)–O(1) length, suggests that residue variation may be expressed for the present purposes in terms of the virtual angles O(1)–C(1)–C(4) and C(1)–C(4)–O(4), hereafter denoted as π_1 and π_2 respectively. Table 1 lists these angles along with related geometric parameters for a number of glucose rings. The forces distorting the rings seem to act on both π_1 and π_2 simultaneously, in concert with changes in the O(4)–O(1) length.

The extent of permitted rotations about the bonds of the glycosidic linkage is most graphically illustrated by two examples, the cyclohexaamylose–water adduct⁴ and the comparison of 6-iodophenyl α -maltoside¹³ with other maltoses^{2,3,18}. The range found in the cyclohexaamylose structure is surprising because of the closed macro-ring. All told, the observed linkage torsion angles ϕ and ψ vary within 60° ranges. Thus, the flexibility of the ring and the variety of observed rotations about the glycosidic bonds give notice that a large variety of amylose conformations should be expected.

THEORY OF HELICAL CONSTRAINTS AS REVEALED BY MODELS OF CYCLODEXTRINS

The virtual-bond method of building polymeric models^{1,19,20}

Table 1 Parameters for glycosidic atoms in α -D-glucose residues

Residue	Reference	Distances (Å)				Angles (degrees)		Torsion angles (degrees)
		O(4)–O(1)	C(1)–C(4)	O(1)–C(1)	C(4)–O(4)	O(1)–C(1)–C(4) (π_1)	C(1)–C(4)–O(4) (π_2)	O(1)–C(1)–C(4)–O(4)
α -Maltose–H ₂ O (non-reducing)	2	4.052	2.879	1.415	1.417	93.6	138.1	–7.1
Cyclohexaamylose–H ₂ O (residue 3)	4	4.106	2.872	1.432	1.433	95.1	138.8	–1.2
Cyclohexaamylose–propanol (residue 1)	5	4.154	2.857	1.415	1.443	96.8	139.9	.4
Trehalose–2 H ₂ O (unprimed)	6	4.208	2.864	1.417	1.411	96.2	144.0	–13.8
Cyclohexaamylose–KAc (residue 3)	7	4.252	2.868	1.417	1.429	99.6	141.5	–1.7
Trehalose–2 H ₂ O (primed)	6	4.332	2.893	1.420	1.411	98.9	146.4	–6.3
<i>iso</i> -Maltulose	8	4.370	2.873	1.397	1.423	100.1	148.0	–6.0
Methyl α -glucoside	9	4.375	2.862	1.412	1.420	101.3	146.8	–11.9
Arnott–Scott average	10	4.400	2.887	1.415	1.426	101.0	147.1	–5.9
α -Lactose–H ₂ O	11	4.455	2.876	1.387	1.436	103.4	148.0	–6.0
α -Glucose–urea	12	4.476	2.889	1.384	1.422	104.4	147.6	–10.3
Phenyl α -maltoside	13	4.478	2.904	1.417	1.425	103.7	147.0	–7.9
Lactose–CaBr ₂	14	4.510	2.898	1.364	1.432	105.5	147.8	–6.5
Glucose–H ₂ O	15	4.513	2.867	1.412	1.435	104.9	149.6	–1.1
Sucrose	16	4.543	2.879	1.421	1.414	106.2	149.4	–12.5
1-Kestose	17	4.575	2.871	1.417	1.435	104.9	153.2	–4.6

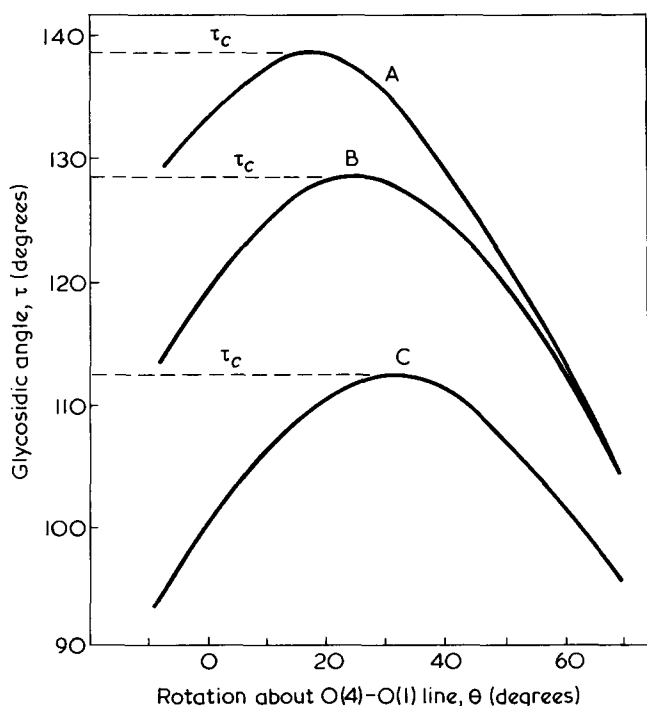


Figure 1 Effect of O(4)–O(1) length on glycosidic angle and τ_c for cyclohexaamylose. The three curves are for residues with short, intermediate and long O(4)–O(1) distances: A, 4.57 Å; B, 4.37 Å; C, 4.05 Å

provides a convenient framework for considering the constraints imposed upon residue geometry by a given helical conformation. Different values of n (number of residues per turn of the helix) and h (rise per residue) cause the angular relationship between neighbouring virtual bonds to be different in the various polymorphs of amylose. In some instances, the polysaccharide can accommodate this angular change by undergoing rotations about the valence bonds to the linkage oxygen atoms. Other examples require a change in glucose ring geometry (specifically the angles π_1 and π_2). Because the role played by the parameter n in constraining residue geometry is especially apparent for helices with zero pitch, the following discussion will consider only sym-

metric models of cycloamyloses. These molecules, the α , β and γ Schardinger dextrans, are understood to be closed rings, or tori, having 6, 7 and 8 α -D-glucose residues.

Computer models of cycloamyloses may be formed by linking together residues with a given geometry. Once their virtual bonds are arranged to construct the appropriate six-, seven-, or eight-sided polygon, the glucose rings may be rotated (equally) about their virtual bonds, resulting in different values for the glycosidic angle. The effect of this rotation (θ) upon the glycosidic angle (τ) is shown in Figure 1 for three residues used to model cyclohexaamylose. The maximum τ or τ_c ¹⁹ achieved by the shortest residue is 112°, whereas that attained by the longest residue is 139°. Because τ_c occurs when all the carbon and oxygen atoms of the linkages are essentially coplanar, Figure 2 can be used to learn how the τ_c values are related to the O(4)–O(1) distances in the residues used to construct the models. Within the approximation of planarity of all the glycosidic atoms, simple geometric arguments demonstrate that $\tau_c = \pi_1 + \pi_2 - \chi$, where $\chi = 180^\circ - (360^\circ/n)$ and is the angle between adjacent virtual bonds in the model.

Recalling that the data in Table 1 showed that π_1 and π_2 steadily decrease with decreases in O(4)–O(1) length, τ_c must also decrease for a given value of χ . Also, because χ increases as n increases, τ_c for a given residue must decrease as n increases. Table 2 shows the values of τ_c for models of the α , β and γ cyclodextrins built from the various actual geometries in Table 1. In every case, τ_c is highest for the six-residue structure and lower by 9° and 15° (exactly the differences in χ) for the seven- and eight-residue structures. Thus, despite use of actual glucose geometries with a 15° range in the O(1)–C(1)–C(4)–O(4) virtual torsion angle, the summation $\pi_1 + \pi_2 - \chi$ always yields τ_c within 1°.

Observed bond angles at the glycosidic linkage have ranged from 116° to 122° in maltose^{2,3,13,18} and cyclohexaamylose²¹ so we expect a similar limited range for other hexaamyloses and the hepta- and octa-amyloses as well. If the computer models are required to possess glycosidic angles of $119^\circ \pm 3^\circ$, an increasing number of the residues are unable to produce models (see Table 2) that would be considered reasonable as the number of residues in the cyclodextrin increases. As shown in Figure 3, θ values lower than or equal to those yielding τ_c are required for all models

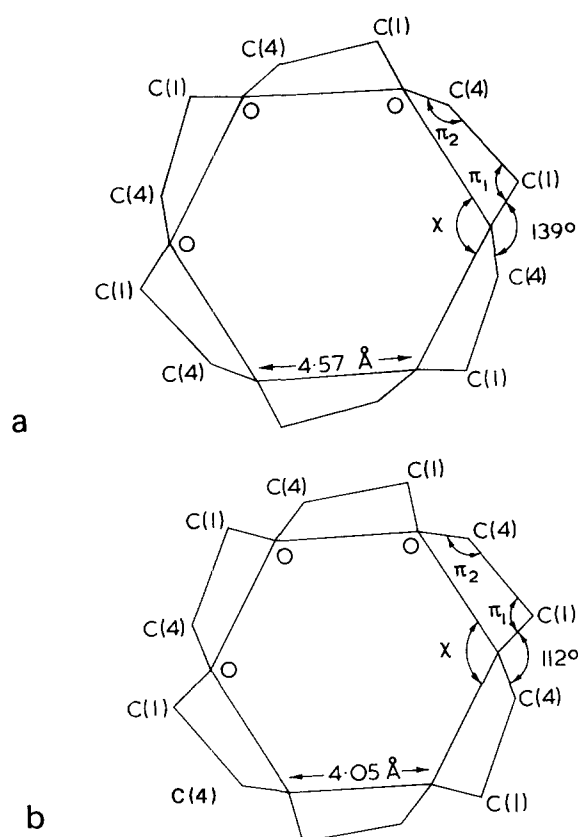


Figure 2 Effect of decreased O(4)–O(1) distance on τ_c in α -cyclohexaamylose. Virtual-bond (computer) models of cyclohexaamylose showing only the linkage oxygen atoms, C(1) and C(4). (a) This model has an O(1)–C(1)–C(4) angle of 105° and a C(1)–C(4)–O(4) angle of 153.2° , resulting in a large maximum glycosidic angle of 139° . (b) The virtual angles have values of 94° and 138° , resulting in a small maximum glycosidic angle of 112° . Because the C(1)–C(4) distances are nearly equal in both models, the differences in the O(1)–C(1)–C(4) and C(1)–C(4)–O(4) angles are responsible for the difference in the O(4)–O(1) distances

due to a territorial conflict between O(2) and O(3') at higher values of θ . Substantially lower values of θ permit the longer residues to form models with reasonable glycosidic angles for the six- and seven-residue species, but then the possibility of an O(2)–O(3') hydrogen bond is sacrificed. Table 2 also indicates (with superscripts) the rather limited ranges of residue geometry that allow reasonable glycosidic angles as well as proposed O(2)–O(3') hydrogen bonds for each of the three structures. This hydrogen bond is likely to be found in the eight-residue cycloamylose because models with too large an O(2)–O(3') distance are unable to attain reasonable glycosidic angles.

Thus, the different values of the helical parameter, n , can require different residue geometries. Table 3 presents predicted parameters for the cyclodextrins based on these modelling studies. Saenger²¹ reports that in ten different cyclohexaamylose crystals (57 determinations of residue geometry), the overall average value for the O(4)–O(1) length is 4.251 Å, with a maximum and minimum average per crystal of 4.307 and 4.211 Å, respectively, in substantial agreement with the results depicted in Tables 2 and 3. The residues of maltose^{2,3} however, are not restricted by the 'helical' constraints and, as cited in the previous section, show much greater variability.

Although some parameters, such as O(6) position, are quite variable, the average glycosidic angle and average O(4)–

O(1) length are nearly constant in the cyclohexaamyloses; moreover, they all exhibit a pronounced tendency to form O(2)–O(3') hydrogen bonds²¹. By adopting different aver-

Table 2 Maximum possible glycosidic angles (τ_c) in computer models of three cyclodextrins

Residue geometry		τ_c (degrees)		
O(4)–O(1) length (Å)	$\pi_1 + \pi_2$ (degrees)	α -Dextrin	β -Dextrin	γ -Dextrin
4.052	231.7	112	103	97
4.106	233.9	114	105	99
4.154 ^a	236.7	117	108	102
4.208 ^a	240.2	121	113	106
4.252 ^a	241.1	121	113	106
4.332	245.3	125	117	111
4.370 ^b	248.1	128	120	113
4.375 ^b	248.1	129	120	114
4.400 ^b	248.1	129	120	114
4.478 ^b	250.7	131	123	116
4.455 ^b	251.4	132	123	117
4.476	252.0	132	124	118
4.510 ^c	253.3	134	125	119
4.513 ^c	254.5	134	126	120
4.543 ^c	255.6	136	128	121
4.575 ^c	258.1	139	130	123

a, b, c Stereochemically reasonable six-, seven- and eight-residue models with O(2)–O(3') hydrogen bonds can be built using these residues

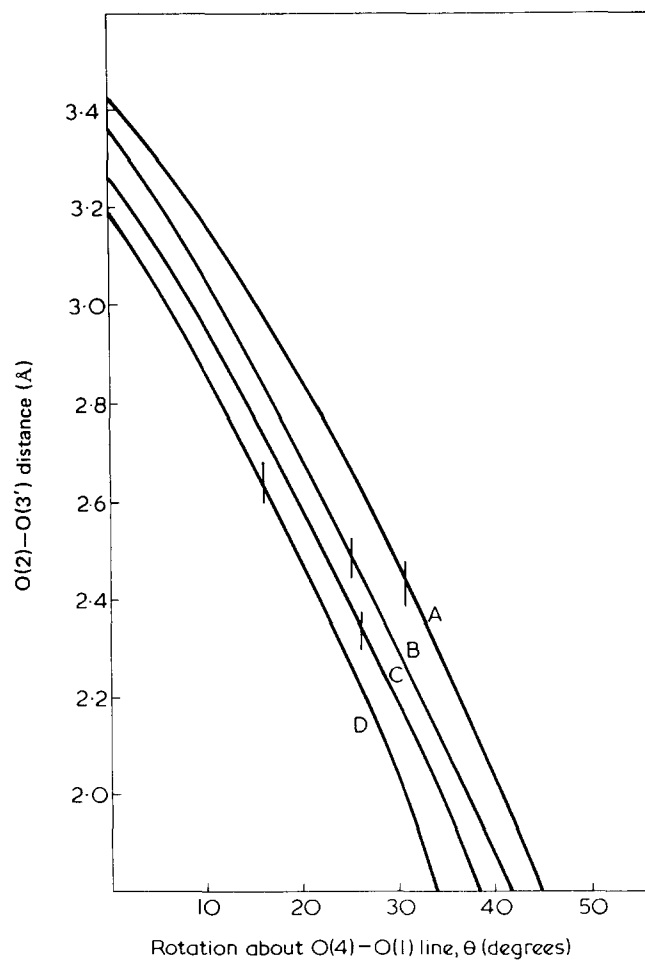


Figure 3 Distances between O(2) and O(3') as a function of rotation about the O(4)–O(1) line. The vertical lines represent the rotations at which the maximum glycosidic angle (τ_c) is possible. If contacts shorter than 2.6 Å are not allowed, then all rotations must be lower than that yielding τ_c . A, 4.05 Å (ref 2); B, 4.37 Å (ref 8); C, 4.25 Å (ref 7); D, 4.57 Å (ref 17)

age residue geometries, models of cyclohepta- and cycloocta-amylose are also able to form hydrogen bonds and maintain reasonable glycosidic angles. A different residue geometry should therefore be characteristic of each of the three sizes of cyclodextrins. There should also be differences in the relative flexibility of the macro-rings. Because the predicted average O(4)–O(1) lengths for cyclohexa- and cyclohepta-amylose are near the median of the observed range, substantially longer and shorter residues could comprise the averages. Indeed, some of the cyclohexaamyloses do show this variability²¹. However, the predicted average length for the residues in cyclooctaamylose is near the upper end of the range; consequently, less variability is expected in this species.

EXTENSIONS TO MODELS OF AMYLOSES

It is not a remarkable conclusion that these same principles should apply to amylose helices. In itself, the differing helical parameter, n , for various polymorphs can require the glucose ring to assume somewhat different average shapes. The helical parameter, h , also influences the required geometry. As h increases towards the limit of the glucose virtual bond length, χ approaches 180° . Therefore, π_1 and π_2 must also increase with h . Table 4 presents results for a number of polymorphs. These polymorphs were all recently reviewed²² in the context of these computer models (shown in Figure 4), so only a brief discussion is given here. The only model that is based on a combined diffraction intensity and stereochemical analysis is that of the six-residue V amylose structure²³. The others are simply based on intrahelical stereochemical considerations¹ (such as shown in Figures 1 and 3) and the fibre repeat spacing and symmetry indicated by the diffraction patterns. All models are left-handed based on the interconvertibility of the polymorphs, the diffraction analyses for V amyloses, and the stereochemistry of the KBr and intermediate amyloses²².

As shown in Table 4, an O(4)–O(1) length of 4.57 Å

characterizes the models of both V₈ amylose which has the shortest h (1.0 Å) and KBr–amylose which has the longest (4.05 Å). In this case, then, the difference between a helix with 8 residues per 8 Å and one with 4 residues per 16.1 Å primarily resides in the linkage conformation angles (note the differences in ϕ and ψ for the two models) with little or no difference in residue geometry. On the other hand, the V₆, V₇ and V₈ models all have approximately the same linkage conformation but their O(4)–O(1) lengths range from 4.25 Å for V₆ to 4.57 Å for V₈, indicating that polymorphic transformations within this group involve significant changes in the residue shape. In general, therefore, a description of macromolecular structure requires a specification of residue geometry as well as θ (or, equivalently, ϕ and ψ) and τ .

The prototype molecules for amylose, the cyclohexaamyloses, often differ substantially from what might be expected from a stereochemical analysis of the isolated molecule. In some instances, however, the real molecules are nearly symmetrical and do approach our models in detail. Accurate determination of amylose structures that are deformed will probably be very difficult because in the deformed cyclodextrins there is little uniformity in modelling parameters such as virtual bond length and glycosidic angle (except as averages)²¹.

To the extent that future determinations of cyclohepta- and cycloocta-amyloses verify the modelling predictions in Table 3, amylose polymorphs should be similar to those proposed in Table 4. The water⁴ and molecular iodine²⁵ cyclohexaamylose complexes already provide evidence of the extent to which residue geometries may differ from the average, owing to irregularity in the molecular backbone. (Incidentally, these particular conformations of the molecules also suggest that greater flexibility of the polymer is possible than might be deduced from handling models such as the space-filling CPK type now in common use.) In the instance of the *p*-iodoaniline–cyclohexaamylose complex, the macro-ring is elliptical owing to insertion of the large, flat iodoaniline molecule²¹. The individual angles between virtual bonds are different and affect the individual residue geometries (specifically, the angles π_1 and π_2) in a manner similar to what we have proposed.

Table 3 Parameters for computer models of cyclodextrins

Residues per cycle	O(4)–O(1) length (Å)	τ (degrees)	ϕ^* (degrees)	ψ^* (degrees)	θ (degrees)	O(2)–O(3') distance (Å)
6	4.25	120	–7	7	20	2.78
7	4.40	119	–4	4	15	2.75
8	4.54	120	–1	6	10	2.88

* Conventions are those described in ref 22

Table 4 Parameters for computer models of amylose polymorphs

Polymorph	Residues/pitch (Å)	O(4)–O(1) length (Å)	τ (degrees)	ϕ^* (degrees)	ψ^* (degrees)	θ (degrees)	O(2)–O(3') distance (Å)
V ₆	6/8	4.25	119	–14	–6	18	2.75
V ₇	7/8	4.41	118	–18	–3	6	2.78
V ₈	8/8	4.57	119	–6	–5	3	2.80
KBr	4/16.1	4.57	120	–60	–41	–53	4.51
KOH	6/22.6	4.57	119	–3	–33	10	2.93
Intermediate	5/19.1	4.53	119	–37	–30	–15	3.79
Native	6/21.0†	4.48	117	–28	–5	–5	3.35

* Conventions are those described in ref 22. † One strand of a double helix

CONCLUSIONS

The simpler task for computer modelling is the description of a particular conformation with known n and h . In this task, the virtual-bond, model-building method^{1,19,20} is advantageous because only models with a given n and h are considered. By utilizing a sufficient range of monomer geometries, it is possible to consider a variety of feasible models with different θ values and thus test the postulated hydrogen

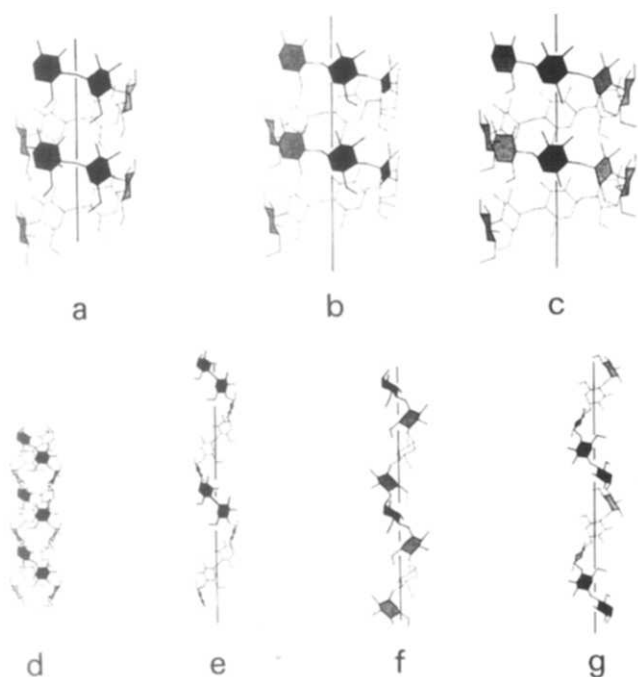


Figure 4 Drawings of amylose polymorphs (For more complete discussion, see ref 22.) (a) Six-residue V amylose. Two recent structure determinations have been performed on this polymorph^{23,24}. The amylose molecule also takes this form in the presence of small alcohols, fatty acids, iodine and dimethyl sulphoxide. (b) Seven-residue V amylose. This polymorph has been proposed to account for the larger unit cell constants obtained when amylose is precipitated with larger agents such as tert-butyl alcohol. (c) Eight-residue V amylose. Still larger precipitating agents yield still larger unit cells with tetragonal symmetry; hence, eight-residue helices have been proposed. Because of the long residue required for this polymorph and also for KBr-amylose and because of the tetragonal symmetry of both species, the symmetric computer models may be more accurate than usual. (d) Native amylose. Fibre patterns that resemble the A and B powder patterns may most reasonably be interpreted in terms of parallel-stranded, double helices. (e) KOH-amylose. The alkali addition forms are very extended helices. Although there are six residues per turn of the helix, the crystal symmetry is only two-fold; therefore, substantial differences in θ could occur from residue to residue. This is possible for the long residue in this case because the glycosidic angle changes more slowly with θ when the virtual bond is nearly parallel to the helix axis²⁰. (f) KBr-amylose. This polymorph has the largest known rise per residue (4.05 Å) among the amyloses; whereas, the eight-residue V helix has the lowest value (about 1.0 Å). Both require similar residue geometry but differ in θ (or ϕ and ψ). (g) Intermediate amylose. Wetting of any of the above polymorphs at room temperature usually results in a sample that gives a B diffraction pattern. Occasionally, however, wetting of the KOH-amylose filaments yields a new pattern instead of the B pattern. The fifth and tenth order meridional reflections are interpreted as indicating this five-residue, extended helix

bonding and other features against stereochemical and diffraction data^{20,23}.

A second topic for computer modelling is a determination of the extent of the allowed conformations for a given chemical composition. The Ramachandran (ϕ , ψ) maps²⁶ used for this purpose^{18,27,28} are inadequate to depict the entire range of allowed conformations. For example, no single map would show all the known cyclodextrins as geometrically allowed because ϕ and ψ are essentially equal in the α , β and γ cyclodextrins. For possibly crystalline conformations, perhaps the best way to describe the allowed range would be a graph of h vs. n , with the feasibility or even potential energy of grid points determined from con-

sideration of the full ranges of glycosidic angle and monomeric geometry.

Because small differences in monomer characteristics result in favourable indications for different polymorphs, it would be tedious to examine comprehensively all possible combinations of n and h by means of our current programs which generate polymeric chains from a rigid residue via the virtual-bond method. This same criticism applies to the preparation of many ϕ , ψ maps for different geometries and glycosidic angles. A program^{10,24} incorporating a flexible monomer with optimization in terms of stereochemistry appears to be a solution. Owing to the systematic nature of the required changes in ring geometry, addition of decision making routines and storage for a range of residue geometries should also enable the virtual-bond method to be used efficiently.

In view of recent advances, questions raised in our earlier paper¹ can be answered. The chief cause of residue variability is its environment, specifically the hydrogen bonding and crystal packing. The largest difference observed in residue geometry occurs for residues that are virtually identical from the standpoint of chemical substitution and that are crystallized with only carbohydrate and water^{2,3}. Extending this argument to polysaccharides, we suggest that environmental factors determine the helical parameters of the crystalline polymer and thereby alter the specific monomeric geometry. Supporting or contradictory evidence for this proposal should result from determinations of the structures of the highly crystalline cyclohepta- and cycloocta-amyloses.

Recent studies have also expanded the range of glucose geometries. The discovery of the especially short glucose residue in α -maltose monohydrate² (0.15 Å shorter than any in our earlier survey¹) enables construction of a reasonable amylose model having five residues per 8 Å repeat, a structure that would have been considered inaccessible with any of the previously available geometries. In view of the earlier work¹, this means that it is currently possible to build reasonable V amylose type models having from five to nine residues per repeat. How much more this range can be expanded depends, of course, upon the as yet undefined limit to the flexibility of the monomeric units. Hopefully, further determinations of single-crystal structures and thorough theoretical studies of ring potential energies will supply the necessary information. Further studies are also needed to explain why only the six-, seven- and eight- residue V amyloses have actually been observed and whether hydrogen bonding and crystal packing considerations are responsible for all the known polymorphs adopting either a collapsed form with $h = 1.0$ – 1.3 Å or a very extended form with $h = 3.5$ – 4.0 Å.

ACKNOWLEDGEMENTS

The authors thank Fusao Takusagawa and Robert Jacobson for furnishing structural data on α -maltose.

REFERENCES

- 1 French, A. D. and Murphy, V. G. *Carbohydr. Res.* 1973, 27, 391
- 2 Takusagawa, F. and Jacobson, R. A. Submitted to *Acta Crystallogr.*
- 3 Chu, S. C. and Jeffrey, G. A. *Acta Crystallogr.* 1967, 23, 1038
- 4 Manor, P. C. and Saenger, W. *J. Am. Chem. Soc.* 1974, 96, 3630
- 5 Saenger, W., McMullan, R. K., Fayos, J. and Mootz, D. *Acta Crystallogr. (B)* 1974, 30, 2019

Changes during amylose transformations: A. D. French and V. G. Murphy

- | | |
|---|--|
| <p>6 Taga, T., Senma, M. and Osaki, K. <i>Acta Crystallogr. (B)</i> 1972, 28, 3258</p> <p>7 Hybl, A., Rundle, R. E. and Williams, D. E. <i>J. Am. Chem. Soc.</i> 1965, 87, 2779</p> <p>8 Dreissig, V. W. and Luger, P. <i>Acta Crystallogr. (B)</i>, 1973, 29, 514</p> <p>9 Berman, H. M. and Kim, S. H. <i>Acta Crystallogr. (B)</i> 1968, 24, 897</p> <p>10 Arnott, S. and Scott, W. E. <i>J. Chem. Soc. Perkin Transactions II</i> 1972, 324</p> <p>11 Fries, D. C., Rao, S. T. and Sundaralingam, M. <i>Acta Crystallogr. (B)</i> 1971, 27, 1969</p> <p>12 Snyder, R. L. and Rosenstein, R. D. <i>Acta Crystallogr. (B)</i> 1971, 27, 994</p> <p>13 Tanaka, I., Tanaka, N., Ashida, T. and Kakudo, M. <i>Acta Crystallogr. (B)</i> 1976, 32, 155</p> <p>14 Bugg, C. E. <i>J. Am. Chem. Soc.</i> 1973, 95, 908</p> <p>15 Hough, E., Neidle, S., Rogers, D. and Troughton, P. G. H. <i>Acta Crystallogr. (B)</i> 1973, 29, 365</p> <p>16 Brown, G. M. and Levy, H. A. <i>Rome IUCr Meeting</i> 1963; For most recent work see <i>Acta Crystallogr. (B)</i> 1973, 29, 790</p> <p>17 Jeffrey, G. A. and Park, Y. J. <i>Acta Crystallogr. (B)</i> 1972, 28, 257</p> <p>18 Quigley, G. J., Sarko, A. and Marchessault, R. H. <i>J. Am. Chem.</i></p> | <p><i>Soc.</i> 1970, 92, 5834</p> <p>19 Sundararajan, P. R. and Marchessault, R. H. <i>Can. J. Chem.</i> 1975, 53, 3563</p> <p>20 French, A. D. and Murphy, V. G. <i>New York ACS Meeting</i> 1976</p> <p>21 Saenger, W. in 'Environmental Effects on Molecular Structure and Properties' (Ed. B. Pullman), D. Reidel, Dordrecht, Holland, 1976, p 265</p> <p>22 French, A. D. and Murphy, V. G. <i>Cereal Foods World</i> 1977, 22, 61</p> <p>23 Murphy, V. G., Zaslow, B. and French, A. D. <i>Biopolymers</i> 1975, 14, 1487</p> <p>24 Zugenmaier, P. and Sarko, A. <i>Biopolymers</i> 1976, 15, 2121</p> <p>25 McMullan, R. K., Saenger, W., Fayos, J. and Mootz, D. <i>Carbohydr. Res.</i> 1973, 31, 211</p> <p>26 Ramachandran, G. N., Ramakrishnan, C. and Sasisekharan, V. in 'Aspects of Protein Structure' (Ed. G. N. Ramachandran) Academic Press, London, 1963, p 121</p> <p>27 Brant, D. A. <i>Ann. Rev. Biophys. Bioeng.</i> 1972, 1, 369</p> <p>28 Goebel, C. V., Dimpfl, W. L. and Brant, D. A. <i>Macromolecules</i> 1970, 3, 644</p> |
|---|--|